J. Fluid Mech. (1981), *vol.* 112, *pp.* 443–458
Printed in Great Britain

Waves in a viscous liquid curtain

By S. P. LIN AND G. ROBERTS
Clarkson College of Technology, Potsdam, New York 13676

(Received 10 November 1980 and in revised form 17 March 1981)

The wave motion created by a small obstacle placed in a viscous liquid curtain which falls steadily between two vertical guide wires is studied experimentally. The disturbances introduced by the obstacle propagate in the curtain to form two distinctive stationary lines of constant phase; one corresponds to the sinuous mode and the other to the varicose mode. The observed wave motion compares very well with that predicted by the theory of Lin (1980). The observed angle between the tangent at any point on the line of constant phase and the vertical are used to infer the dynamic surface tension of a rapidly moving surface. A considerable difference between the dynamic surface tension and the usual static surface tension is found for a liquid solution. However, no measurable difference is found for a pure liquid at the flow rates used in our experiments.

1. Introduction

The dynamics of thin sheets of liquids is of considerable scientific and technological importance. The subject was studied as long ago as 1833 by Savart. Several early works in this area were discussed by G. I. Taylor (1959, 1960) in his extensive investigations of the subject. Some of the more recent works on the topic in connection with atomization, combustion, spray coatings, and curtain coatings are referenced in the recent work of Lin (1980). By use of linear theory, Lin investigated the stability of a thin sheet of viscous liquid flowing between two vertical guide wires. He showed that the disturbances can be separated into varicose and sinuous waves. The varicose waves are always damped but the sinuous waves, when their group velocity is directed upstream, are responsible for the curtain instability. The group velocity tends to propagate upstream only when the Weber number of the curtain flow exceeds $\frac{1}{2}$. The predicted critical Weber number agrees completely with that found experimentally by Brown (1961). He observed that a stable liquid curtain can be formed only if the Weber number is below $\frac{1}{2}$. When the Weber number is raised beyond this critical value, by reducing the discharge rate for example, the liquid curtain disintegrates.

In the present work, we show that, if disturbances are introduced continuously into a stable liquid curtain, the sinuous and varicose waves predicted by Lin will sort themselves out to form two distinctive stationary lines of constant phase. The predicted stationary wave fronts compare very well with experimental observations based on two different techniques. Easily measurable geometric properties of the stationary waves are then used to infer the dynamic surface tension of rapidly moving liquid surfaces. The considerable difference between the surface tension of a moving liquid solution and that of the same liquid in a thermodynamic equilibrium has been demonstrated.

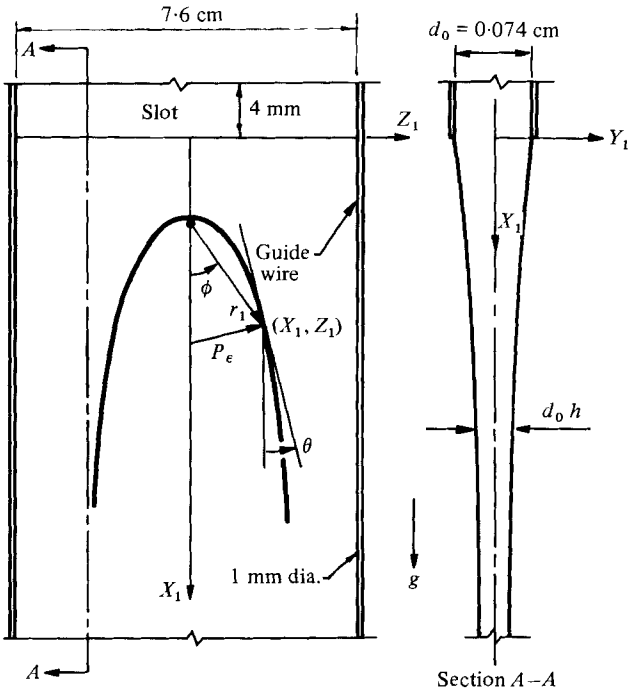

FIGURE 1. Definition sketch.

2. Curtain waves

Consider the steady flow in the Newtonian liquid curtain shown in figure 1. Brown (1961) gave the following empirical equation for the average velocity distribution along the curtain

$$U_1^2(X_1) = (Q/d_0)^2 + 2gX_1 - C(4\nu g)^{\frac{2}{3}}, \tag{1}$$

where U_1 is the average velocity in the direction of the Cartesian co-ordinate axis X_1 which has the same direction as the gravitational acceleration g, Q is the volumetric flow rate per unit width of the curtain, ν is the kinematic viscosity, C is a constant and d_0 is the maximum curtain thickness. In terms of the dimensionless variables defined by $U_1 = (4\nu g)^{\frac{1}{3}}U$ and $X_1 = (4\nu)^{\frac{2}{3}} g^{-\frac{1}{3}}X$, (1) can be written as

$$U^2(X) = U^2(0) + 2X - C.$$

Brown found that the local bulk velocity given by this equation compares very well, except near the slot, with that predicted by a nonlinear differential equation derived by G. I. Taylor and equally well with Brown's own experiments if C is chosen to be 4. Brown observed that, when Q is reduced to a value such that the Weber number of the flow becomes less than $\frac{1}{2}$, the curtain will distintegrate. The Weber number is defined by

$$W = Td_0/\rho Q^2,$$

where T is the surface tension, and ρ is the fluid density. This critical Weber number has been confirmed theoretically by Lin (1980) who applied linear stability analysis to a liquid curtain of a small thickness such that

$$\delta = (g^2/4\nu)^{\frac{1}{3}}(d_0^2/Q) \ll 1.$$

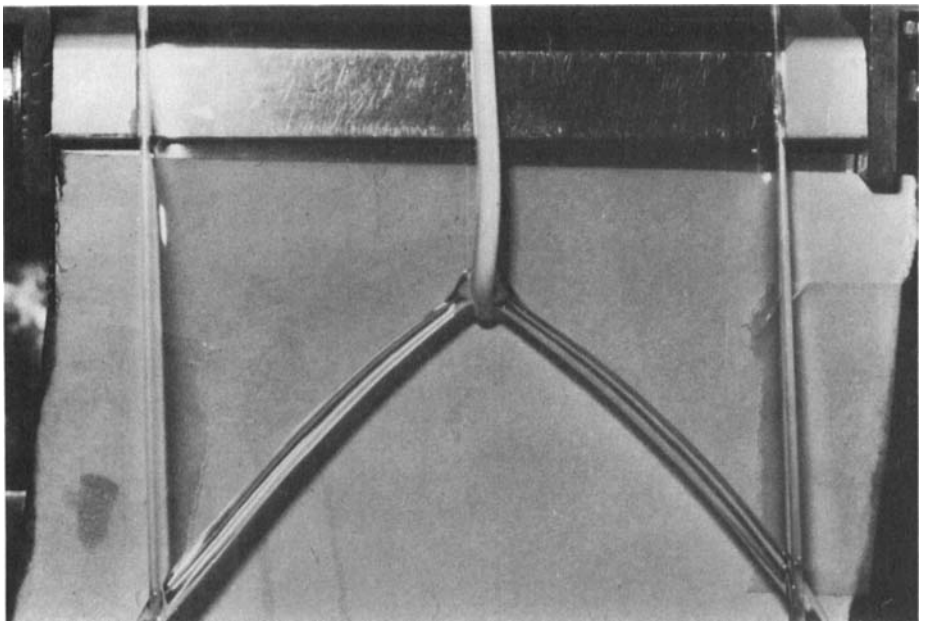

FIGURE 2. Free edges created by an obstable.

For such a curtain Lin showed that the flow is locally parallel, to the first-order approximation, and the detailed knowledge of the velocity variation given by (1) is not needed in the linear stability analysis. The above inequality is satisfied by most of the liquid curtains encountered in our experiments to be described shortly.

Brown also reported that a stable curtain with $W < \frac{1}{2}$ can be broken to form an inverted V-shaped free edge by poking completely through the curtain with an obstacle as shown in figure 2. However we found that if a wettable rod is placed into the curtain carefully enough to avoid the meeting of the two free surfaces, the curtain will not break. In place of the free edge a set of stationary waves now appears on the curtain as shown in figure 3. We show presently that these wave patterns can be predicted by use of the results of Lin's stability analysis.

Lin showed that there exist two independent modes of wave motion in a liquid curtain. One mode is sinuous and the other is varicose. The disturbances which displace the two free surfaces locally in the same direction perpendicular to the plane of the page create the sinuous waves. The disturbances which symmetrically displace the two free surfaces in the opposite directions create the varicose waves. More general disturbances may be constructed from the superpositions of all Fourier components of these two modes. The wave characteristics of the varicose and sinuous modes are governed respectively by the dispersion equations (13) and (17) of Lin's work (henceforth referred to as I). In a stable curtain such that $W < \frac{1}{2}$, both modes of disturbances of small amplitudes decay exponentially. According to the numerical solutions of (13) and (17) in I, the exponential decay rates decrease with the wavelength. Therefore longer waves are more readily observable. Hence, for the purpose of describing the observed wave fronts, we need only the asymptotic solution of (13) and (17) in I for long waves.

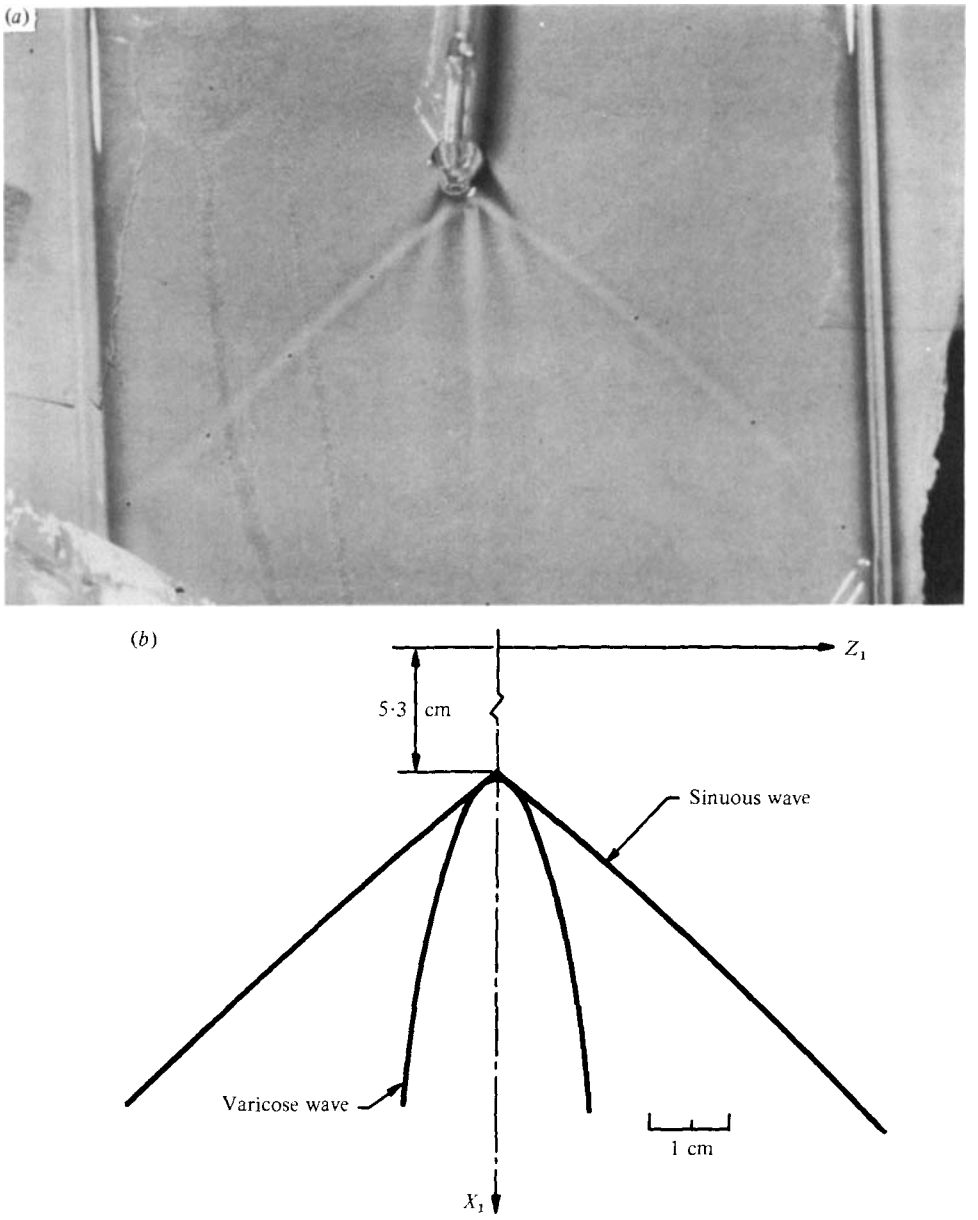

FIGURE 3. Stationary waves in a gelatine solution at 40·6 °C, flow rate 21·3 cm³/s; the distance between the lower edge of the coating lip and the obstacle is 5·3 cm, (*a*) photograph, (*b*) theoretical curve drawn on the same scale as photograph.

2.1. *Sinuous waves*

The asymptotic solution of (17) in I for two-dimensional long sinuous waves propagating along the curtain length is given by (18) of I, i.e.

$$c_r = \bar{u} \pm (2W/h)^{\frac{1}{2}} + O(\alpha^2), \tag{2}$$

$$\alpha c_i = -(h^2/6R)\,\alpha^4, \tag{3}$$

where c_r and $\bar{u}$ are respectively the wave speed and the local curtain velocity both in the unit of $\bar{u}_0 = Q/d_0$, h is the local curtain thickness non-dimensionalized with d_0, αc_i is the exponential decay rate in the unit of $\bar{u}_0/d_0$, and α and R are respectively the wavenumber and the Reynolds number defined by

$$\alpha = 2\pi d_0/\lambda, \quad R = \bar{u}_0 d_0/\nu,$$

where λ is the wavelength.

According to (2) the sinuous wave is nondispersive to the first-order approximation, and its speed relative to the moving fluid is $\pm(2W/h)^{\frac{1}{2}}$. The plus and minus signs correspond to the waves propagating respectively in the downstream and the upstream directions. Only the upstream-propagating waves can be held stationary in space. Along the stationary wave fronts appearing in figure 3, the speeds of the upstream-propagating waves are just balanced by the local fluid velocity component normal to the wave fronts. Thus, along a given phase of the stationary wave, we must have

$$U_1 \sin(\pm\theta) = \pm(Q/d_0)(2W/h)^{\frac{1}{2}} \quad (0 \leqslant \theta \leqslant \pi),$$

i.e.

$$\sin\theta = (2T/\rho Q U_1)^{\frac{1}{2}}, \tag{4}$$

where θ is the angle between the tangent at any point on the stationary wave front and the vertical. In the Cartesian co-ordinates $(x, z) \equiv (X_1, Z_1)/d_0$ the condition (4) can be written as

$$\frac{dz}{dx} = \pm\left(\frac{2T}{\rho Q U_1 - 2T}\right)^{\frac{1}{2}}.$$

The solution of this differential equation with the boundary condition $z = 0$ at $x = m$ is

$$z = (2W)^{\frac{1}{2}}\left(\frac{Q^2}{g d_0^3}\right)[\tfrac{2}{3}\{f^{\frac{3}{2}}(x) - f^{\frac{3}{2}}(m)\} + 4W\{f^{\frac{1}{2}}(x) - f^{\frac{1}{2}}(m)\}], \tag{5}$$

where

$$f(x) = \left[1 - C\left(\frac{d_0}{Q}\right)^2 (4\nu g)^{\frac{2}{3}} + 2g\left(\frac{d_0}{Q}\right)^2 x d_0\right]^{\frac{1}{2}} - 2W,$$

and m is the distance between the y axis and the point where the two branches of the stationary wave meet. m will be taken from the experiment as it cannot be predicted by use of the present results based on the linear theory.

2.2. *Varicose waves*

The dimensionless speed and damping rate of long varicose waves are obtained in I. They are respectively given by

$$\left.\begin{aligned} &c_r - \bar{u} = \pm\alpha\left[\tfrac{1}{2}Wh - \left(\frac{2}{R}\right)^2\right]^{\frac{1}{2}} \quad \text{and} \quad \alpha c_i = -\frac{2}{R}\alpha^2, \quad \text{if} \quad \frac{Wh}{2} - \left(\frac{2}{R}\right)^2 > 0, \\ \text{or} \\ &c_r = \bar{u} \quad \text{and} \quad \alpha c_i = -\frac{2}{R}\alpha^2 \pm \alpha^2\left[\left(\frac{2}{R}\right)^2 - \frac{Wh}{2}\right]^{\frac{1}{2}}, \quad \text{if} \quad \frac{Wh}{2} - \left(\frac{2}{R}\right)^2 < 0. \end{aligned}\right\} \tag{6}$$

It is obvious from (6) that stationary varicose waves can be observed only when $Wh/2 > (2/R)^2$. Comparing the damping rates given in (3) and (6) we expect that it will be more difficult to observe the varicose waves than the sinuous ones, since the former is more rapidly damped. Moreover, the varicose waves are dispersive. It is more

difficult to obtain the curves of constant phase for this mode. We use here the approximate method of Rayleigh (1893).

The varicose waves are held stationary for the same reason the sinuous waves are. Thus, along a given phase of the stationary varicose waves, we have

$$U_1 \sin(\pm\theta) = \pm\left(\frac{Q}{d_0}\right)\left(\frac{2\pi d_0}{\lambda}\right)\left[\frac{Wh}{2}-\left(\frac{2}{R}\right)^2\right]^{\frac{1}{2}} \quad (0 \leqslant \theta \leqslant \pi). \tag{7}$$

The stationary wave is the envelope of varicose waves of different wavelengths λ but of the same phase $\epsilon-\epsilon_0$, where ϵ_0 is a constant reference phase. λ and $\epsilon-\epsilon_0$ are related by (cf. figure 1)

$$\lambda = 2\pi P_e/(\epsilon-\epsilon_0), \tag{8}$$

where P_e is the distance measured normally from any point on the curve of constant phase to the line of sources which produce waves. The line of wave source in the present problem is the centreline of the wake behind the obstacle shown in figures 1 and 3. The phase at this centreline will be referred to as ϵ_0. In the polar co-ordinates (r,ϕ), as shown in figure 1, P_e is given by

$$P_e = d_0\, r \sin\phi/\cos\theta, \tag{9}$$

where r is the radial distance r_1 measured from the centre of the obstacle divided by d_0. Substituting (8) and (9) into (7), we have

$$r\sin\phi\tan\theta = (\epsilon-\epsilon_0)\left[\frac{W}{2\bar{u}^3}-\left(\frac{2}{R}\right)^2\frac{1}{\bar{u}^2}\right]^{\frac{1}{2}}.$$

This equation can be written in the Cartesian co-ordinates as

$$z\frac{dz}{dx} = (\epsilon-\epsilon_0)\left[\frac{W}{2\bar{u}^3}-\left(\frac{2}{R}\right)^2\frac{1}{\bar{u}^2}\right]^{\frac{1}{2}}. \tag{10}$$

Consider a set of n curves of constant phase each corresponding to a stationary wave crest. Then $\epsilon-\epsilon_0 = 2n\pi$ and (10) can be integrated to give

$$z^2 = 4n\pi\int_{x_n}^{x}\left[\frac{W}{2\bar{u}^3}-\left(\frac{2}{R}\right)^2\frac{1}{\bar{u}^2}\right]^{\frac{1}{2}}dx, \tag{11}$$

where x_n is the distance measured from the origin along the x-axis to the apex of each curve of constant phase. It should be pointed out that (11) may not be an accurate description in a region upstream of the obstacle where $\theta \to \frac{1}{2}\pi$ and $\phi \to \pi$. It follows from the definition of α, (8) and (9) that in this region

$$\alpha = \frac{d_0}{P_e}(\epsilon-\epsilon_0) \sim \frac{\epsilon-\epsilon_0}{r}.$$

Thus if the stationary wave crests cut the x-axis at small r such that $2n\pi/r$ is not small, then the condition $\alpha \ll 1$ which was used to arrive at (11) is violated. In this region the complicated full dispersion relation (13) given for finite α in I must be used. However, short waves are so rapidly damped that it would be difficult to observe in practice. It should also be pointed out that the lower integration limit x_n in (11) must be provided from experiment, as it cannot be determined precisely with the present linear theory. Note that, if the curtain thickness were uniform, the integrand in (11) would have been a constant and the resulting curves of constant phase would have formed a set of parabola of focal lengths $n\pi[W/2-(2/R)^2]^{\frac{1}{2}}$.

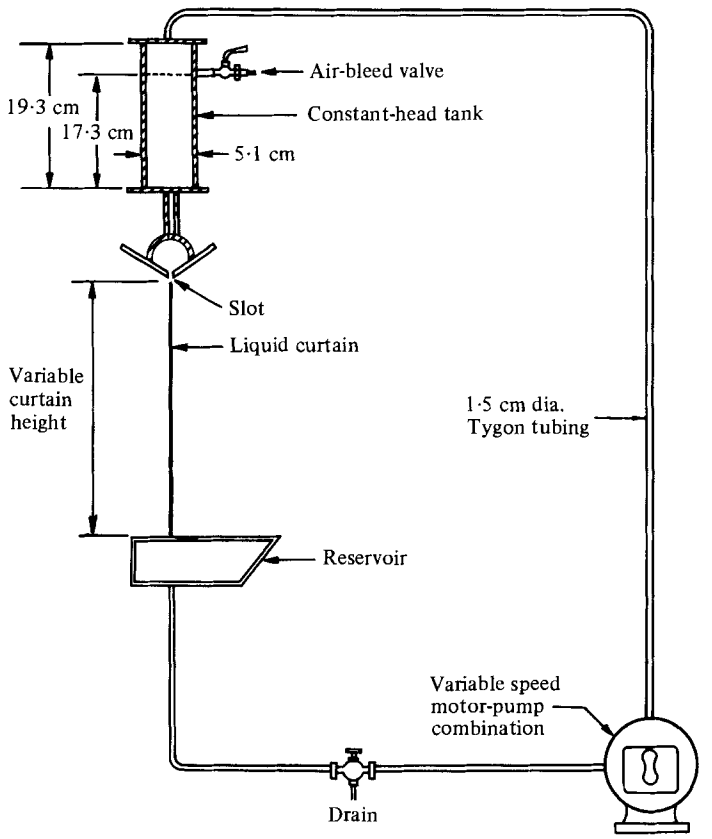

FIGURE 4. Apparatus for producing a curtain of glycerine.

3. Experiments with glycerine

The purpose of the experiment is to observe the stationary wave fronts in a liquid curtain predicted by the theory. As the wave patterns depend crucially on the curtain velocity distribution, the latter must also be accurately measured. The confirmed wave properties will then be used as the basis for dynamic surface tension measurements.

3.1. *Experimental technique*

To produce a steady flow in a vertical thin sheet of liquid, a slot of length 7·6 cm, depth 0·4 cm and width 0·074 cm was constructed and a system for pumping liquid through it built up as shown in figure 4. This apparatus is a slight modification of the system used by Brown (1961). The glycerine of known density, viscosity, surface tension and temperature is pumped through the slot from a reservoir by a pump which was coupled to a variable-speed motor. The density is determined by a hydrometer, viscosity by a falling-ball viscometer and the surface tension by a Rosano surface tensiometer. The liquid leaving the slot is guided by two vertical wires of 0·1 cm diameter. These wires are 7·6 cm apart and are attached to the slot. The liquid curtain formed between these two wires is the test section. The curtain flow reaches steady state when the liquid level in the constant-head tank ceases to fluctuate. The steady volumetric discharge rate is determined as the quotient of the total liquid volume collected in a flask to the time of

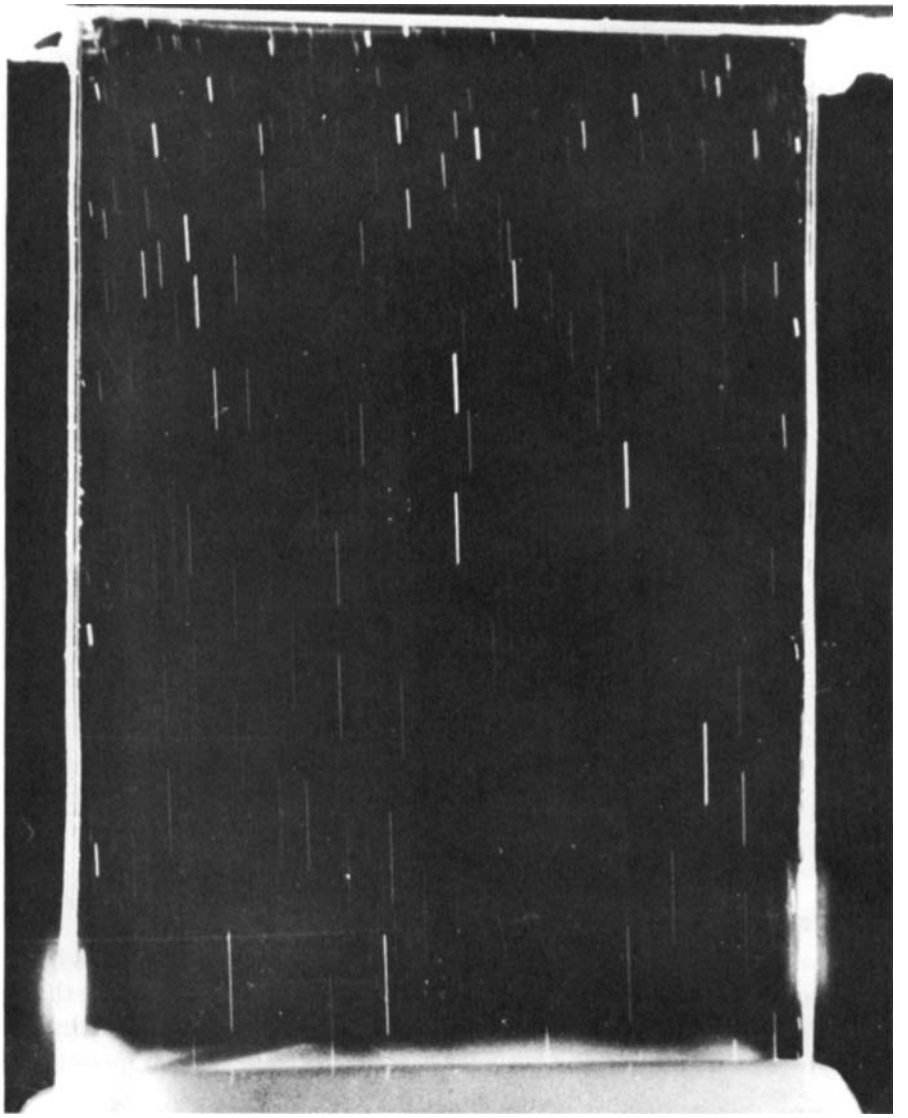

FIGURE 5. Photograph of entrained bubbles for velocity determination. Shutter speed 1/125 s, glycerine temperature 27 °C, flow rate 27 cm³/s.

collection. Flexible Tygon tubings of 1·57 cm diameter are used to connect the constant-head tank and the collection reservoir to the pump.

To measure the local curtain velocity, we allow sufficient numbers of bubbles to be entrapped in the fluid to be used as markers. The bubble entrainment can be achieved by first opening a valve near the top of the constant-head tank, and closing it when the level of the glycerine was near the valve. The pump motor speed was then reduced to a preselected setting, with care being taken to maintain a steady curtain. The bubbles are illuminated by a 500 W projection lamp directed obliquely at the curtain from the front. Still photographs of bubbles are taken from the back of the curtain with sufficiently slow camera shutter speed so that the motion of the bubbles appear as

X_1 (cm)	For flow rate 27 cm³/s		For flow rate 54 cm³/s	
	Experimental	Equation (1)	Experimental	Equation (1)
1	32	28.8	55	43·4
2	50	52·8	63	62·0
3	64	68·9	78	76·1
4	77	81·9	85	88·1
5	93	93·1	94	98·6
6	98	103·1	104	108·1
7	107	112·2	110	116·8
8	115	120·6	119	124·9

TABLE 1. Experimental and theoretical values of U_1 in cm/s.

short streak lines on the photographs. Typical bubble streaks can be seen in figure 5. The lengths of bubble streak lines are either measured directly from the photograph or from the projection of the photograph on a screen. The ratio of the length of any bubble streak line to the camera shutter time then gives the average local curtain velocity at the centre of the streak line in the curtain. This method will yield accurate average curtain velocity if the velocity across the curtain thickness does not change measurably. It will be shown in the next section that this was indeed the case. The shutter speed used was $\frac{1}{125}$ second. This was thought to be the best compromise between a longer time which offers a better time resolution but a poorer spatial resolution associated with the longer bubble trace and a shorter time which offers a better spatial resolution but a poorer time resolution.

The stationary wave pattern was produced by sticking an aluminium rod of 0·32 cm diameter through the liquid curtain at the mid-width. For the photographing of the standing waves, illumination was provided by a small desk lamp placed in front of the curtain and adjusted to produce the maximum contrast between the wave and the rest of the curtain. Some effort was made to align the axis of the camera lens perpendicularly to the liquid curtain, thereby minimizing error due to parallax. The angle between the tangents to the stationary waves and the vertical are either measured directly from the photographs or from the projection of the photograph on a screen.

3.2. *Results*

Three different discharge rates of 27, 36 and 54 cm³/s were used to form a stable glycerine curtain. The temperature of glycerine was 27 °C for the two lower discharge rates and was 31 °C for the largest discharge rate. The measured density, viscosity and surface tension were respectively 1·26 gm/cm³, 8·1 poise and 65·3 dynes/cm at 27 °C, and 1·25 gm/cm³, 5·76 poise and 65 dynes/cm at 31 °C. Typical results of velocity measurements are given in table 1. The values of local velocity calculated from (1) are also given in the same table. The comparison is very good except in the region near the slot. For the lower discharge rate of 27 cm³/s, C in (1) was chosen to be 4 which is the same constant chosen by Brown. However, C was found to be 13·5 and 7, respectively, for the best fit between (1) and the experimental results for the cases of 54 cm³/s and 36 cm³/s. Certainly C is not a universal constant but is dependent on the initial curtain velocity $U(0)$. The values of T mentioned earlier in this paragraph and the measured values of U_1, instead of the calculated ones, were used in determining θ from (4). Some typical results of the angle measurements are given in table 2. A typical

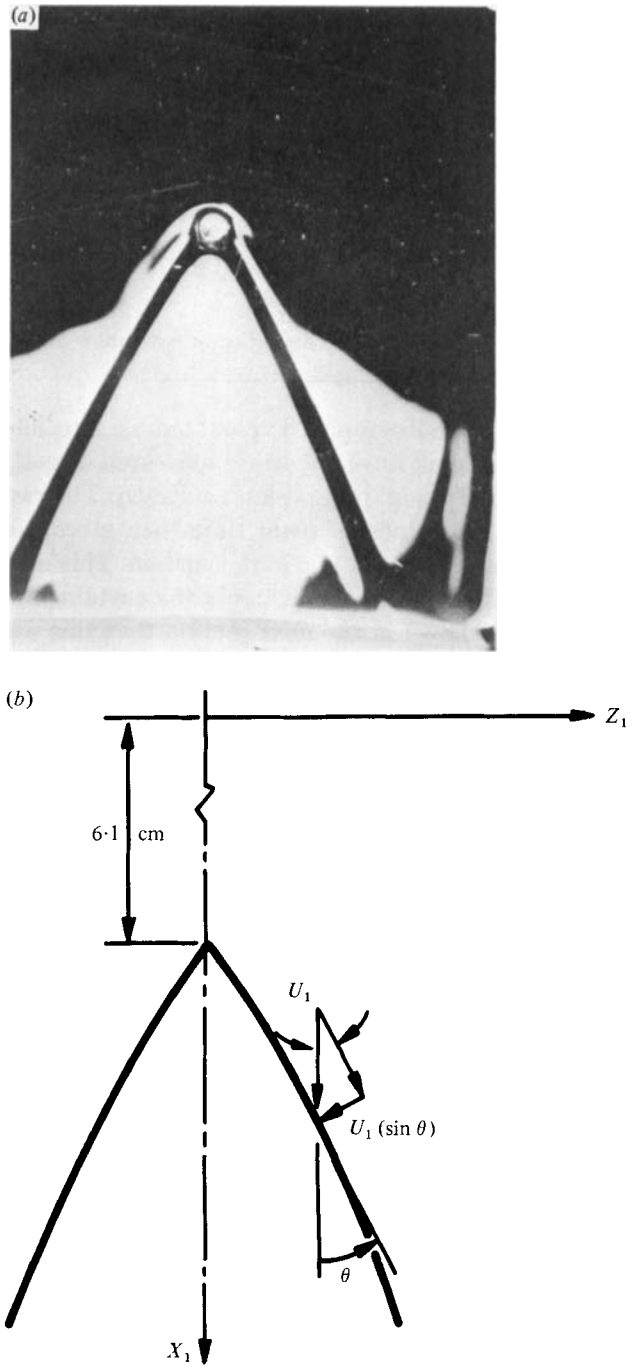

FIGURE 6. Stationary waves in glycerine curtain at 27 °C, 36 cm³/s, the distance between the slot and the obstacle is 6·10 cm, (*a*) photograph, (*b*) theoretical curve drawn on the same scale as photograph.

Flow rate (cm^3/s)	X_1 (cm)	U_1 (cm/s)	Calculated θ (degrees)	Measured θ (degrees)
27	6·7	104	32·0	32·0
27	7·6	112	30·7	30·3
36	6·9	104	27·4	28·5
36	7·5	109	26·6	27·0
36	8·1	114	26·0	26·3
36	8·8	121	25·2	25·5
54	8·6	122	20·2	21·8
54	9·5	129	19·7	21·3
54	10·5	136	19·2	20·0

TABLE 2

photograph of the stationary wave is given in figure 6 (*a*). The curve of constant phase obtained from (5) with U_1 given by (1) and $C = 7$ is, after being converted into a dimensional form, given in figure 6 (*b*). Only sinuous waves are visible in this experiment. It is seen from (3) and (6) that the varicose waves are more rapidly damped than the sinuous ones. It appears that the varicose waves are so quickly damped in the highly viscous glycerine that when their wave crests meet at the line of constant phase they are too faint to be visible. However, they do appear in less viscous fluids as is shown in the next section.

Equation (4) can also be used to determine the surface tension of a rapidly moving liquid which may be considerably different from that of a stagnant liquid. Substituting the measured values of θ, Q, U_1 and ρ as input into (4), we determined the so-called dynamic surface tension. The dynamic surface tension we found differs from the static surface tension we measured by use of the Rosano surface tensiometer only by 5 % which is within the limit of our experimental error. Thus, it appears that there is no measurable difference between dynamic and static surface tension for a pure liquid. This is actually not surprising, since the relaxation time of glycerine molecules in a falling curtain is much shorter than the lifetime of each element of moving surface on a curtain so that each surface is essentially in a thermodynamic equilibrium during its residence time. However, there is a significant difference between the dynamic and the static surface tensions of liquid solutions as will be shown in the next experiment.

It should be pointed out that the condition for the validity of Lin's analysis, i.e. $(g^2/4\nu)^{\frac{1}{3}}(d_0^2/Q) \ll 1$, is satisfied in the above experiments. Our experiments also confirmed the critical Weber number of $\frac{1}{2}$ which was found experimentally by Brown (1961) and predicted recently by Lin (1980) for thin liquid curtains such that $\delta \ll 1$.

4. Experiments with gelatin solution

4.1. *Experimental technique*

The general layout of the present experiments is given in figure 7. A gelatin solution is pumped from a tank to an inclined plane where it is distributed evenly across the width with a slot. At the end of the incline is attached a vertical plate 9·7 cm in width and 1·4 cm in height. The liquid flows under the action of gravity over the incline and the attached vertical plate and is then guided by two vertical rods of 0·1 cm diameter to form a liquid curtain. The liquid leaves the guidance of the vertical rods to form a

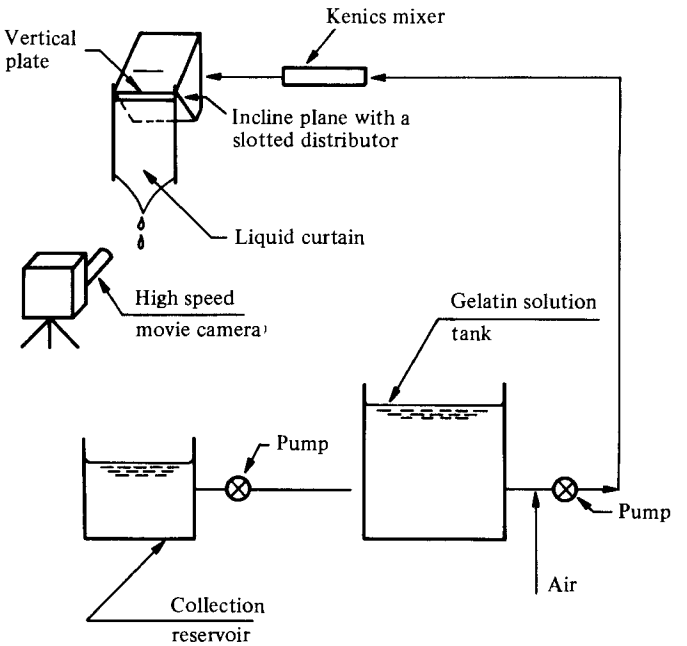

FIGURE 7. Apparatus for producing a curtain of gelatin solution.

V-shaped free edge before falling into a collection reservoir. The liquid is then pumped to the gelatin solution tank to complete a loop.

The velocity of the curtain was measured at different curtain lengths and at locations sufficiently far from the guide rods. In order to measure the bulk curtain velocity, air was introduced slowly from an air compressor into the gelatin solution before it was pumped to the inclined plane, as shown in figure 7. This procedure produced small bubbles which were further reduced in size by a Kenics static mixer.† The micro-bubbles produced by this technique varied in size with a large enough population in the range of 50–150 μm, which is sufficiently smaller than the curtain thickness. The velocity was measured by taking high-speed photographs at about 4000–5000 frames/s. The vertical field of view ranged from 0·8 to 0·84 cm. The distance travelled by the bubble was plotted versus the time of travel, and the velocity was calculated by graphically measuring slopes.

In order to measure surface velocities and compare them with the bulk velocities, polyethylene particles (polythene FN 500) were sprinkled on the surface as tracers. particles were observed to adhere to the surface and thus should reveal the actual surface velocity. Sprinkling the particles on the front surface was a simple task as the front surface of the curtain is formed early on the inclined plane. Adding the particles to the back surface of the curtain was more complicated and a syringe was used to eject the particles onto the back surface as it was formed. The method of measuring the surface velocity is identical with that of measuring the bulk velocity except that the tracer is different.

The stationary wave pattern was produced by sticking a glass rod of 0·15 cm

† Brock, Esley, Inc. 445 East 2nd South, Salt Lake City, Utah 84111.

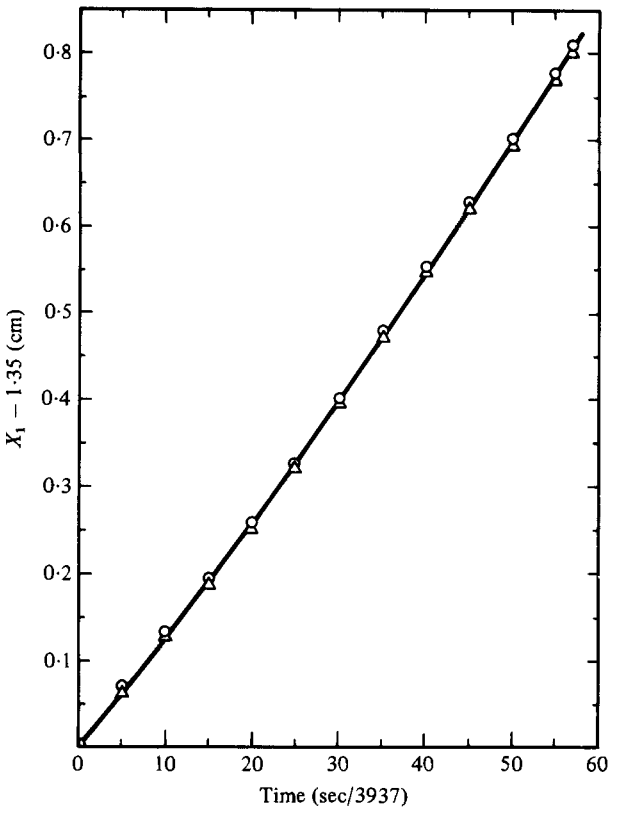

FIGURE 8. Distance plotted against time travelled. ○, 116 μm bubble; △, 89 μm surface particle.

diameter through the liquid curtain. The stationary wave patterns were observed with the same method described in the previous section.

4.2. *Results*

The test fluid was a 12 % gelatin solution of 40·6 °C, which is a Newtonian fluid for shear rates much smaller than 2000 s^{-1}. The density determined as the ratio of the weight to the volume of a given solution was 1·03 g/cm^3. The viscosity and the surface tension measured respectively with a falling-ball viscometer and the Wilhelmy surface tensiometer were 35 cP and 45 dynes/cm. The curtain discharge rate was 21·3 cm^3/s. Typical results of the distance travelled by tracers against time used in the velocity measurements are given in figure 8. The experimentally determined curtain velocities at various locations are given in table 3. The initial curtain velocity was 16 cm/s. The local curtain velocities predicted by Brown's equation (1) with $C = 4$ and by the free fall equation are also given in the same table. At very small curtain lengths, the free fall velocity was about 15 % higher but Brown's equation predicts values only about 6 % higher than the measured velocity. At locations with large curtain lengths, the agreement between the measured velocity and velocity predicted (1) is excellent.

Measuring the slopes of the two curves which pass through the two set of data points in figure 8, we see that the difference between the surface and the bulk velocities, being

X_1 (cm)	U_1 (cm/s) Measured	Equation (1)	Free fall	d (μm)	$2T/\rho QU_1$	δ
1·47	48·7	51·7	56·1	448	1·22	0·082
2·27	62·7	65·1	68·6	348	0·95	0·049
4·73	93·1	95·2	97·6	235	0·64	0·023
5·56	102·3	103·4	105·6	213	0·58	0·019
10·16	139·6	140·4	142·0	156	0·42	0·010
10·99	147·5	146·0	147·7	148	0·40	0·009

TABLE 3

smaller than the experimental error of about 5 %, is negligible. This supports the approximation used by G. I. Taylor in his derivation of a nonlinear differential equation governing the velocity variation along the curtain (see the appendix in Brown's paper).

Both sinuous and varicose waves are observed in this experiment. A typical wave pattern is shown in figure 3. The sinuous wave is more easily visible as it is less damped. Some typical values of the measured θ for the sinuous mode are given in table 4, together with the corresponding measured local velocities and the values of θ calculated from (4) using the static value for T. The measured values of θ are larger than the calculated ones by about 20 % which is more than twice the estimated experimental error bound of about 10 %. This strongly suggests that the surface tension of a rapidly moving surface may differ considerably from that of a stationary surface. Assuming this conjecture to be true, we calculate the dynamic surface tension from (4) with the measured quantities ρ, Q, U_1 and θ for the sinuous wave as input. The values of T thus calculated are given in table 4. Note that the inferred dynamic surface tension is about one and half times larger than the static tension of 45 dynes/cm obtained under a thermodynamic equilibrium situation. We conjectured that this is because the gelatin molecules act as surfactants to lower the surface tension (Antoniades & Lin 1980). It appears that the time required for the gelatin molecules to diffuse and adsorb at the curtain surface before reaching the equilibrium concentration is considerably longer than the residence time of the curtain surface. Consequently, the surface concentration of gelatin is considerably lower than that at equilibrium, when the surface tension reaches its minimum static value. If the surface solute concentration is indeed the main cause of the difference in the two surface tensions, then the dynamic surface tension will depend mainly on the curtain location and thus only on the local surface velocity in a given liquid curtain, but will not depend on the mode of disturbances. The wave patterns calculated from (5) and (11) respectively for the sinuous and varicose modes, with T taken to be the dynamic surface tension inferred from the sinuous wave relation (4), are given in a dimensional figure 3(*b*). Agreements appear excellent for both wave modes. This appears to support our conjecture. The significant difference between dynamic and static surface tension of solutions has also been found by Thomas & Potter (1975). Although their solute and flow differ from ours, the difference they found is of the same order of magnitude as ours.

Local values of twice the Weber number, i.e. $2T/\rho QU_1$, and the local thin curtain parameter $\delta \equiv (g^2/4\nu)^{\frac{1}{3}}(d^2/Q)$ are also listed in table 3. At $X_1 = 0$, $U_1 = 16{\cdot}2$ cm and $d_0 = 0{\cdot}1356$ cm; thus $2W_e = 3{\cdot}66$ and $\delta = 0{\cdot}7476$ at $X_1 = 0$. Apparently the values of

X_1 (cm)	U_1 (cm/sec) Measured	U_1 (cm/sec) Equation (1)	d (μm)	θ (degrees), equation (4) using static T	θ (degrees), measured	T (dynes/cm) equation (4)
1·7	53.5	55.7	410	59·8	No wave	—
5.3	100·0	100·8	220	39·2	50	66
9·4	134·5	134·9	163	33·1	42	68

TABLE 4

δ at $X_1 = 0$ and 1·47 cm do not satisfy the condition of validity of Lin's analysis, i.e. $\delta \ll 1$. This is the reason why the local Weber numbers there exceed the predicted critical Weber number and yet the curtain is still stable. It appears that the rapid change of thickness in the region $X < 1{\cdot}47$ is a stabilizing factor. Although the flow is expected to be unstable in this region, disturbances do not grow very much before they are advected into a region where they decay. To verify this conjecture based on experimental facts, one must carry out the stability analysis for thick liquid curtains for which δ is not small.

5. Conclusion

Our experiments confirm the critical Weber number of $\frac{1}{2}$ which was found experimentally by Brown (1961) and predicted by Lin (1980) only for thin liquid curtain such that $(g^2/4\nu)^{\frac{1}{3}}(d_0^2/Q) \ll 1$. This thin curtain condition was used in Lin's stability analysis and was implied in G. I. Taylor's basic flow derivation. For thick liquid curtains the critical Weber number predicted by Lin is conservative. Stability analyses and corresponding experiments for thick liquid curtains may contribute to a better understanding of the behaviour of viscous liquid sheets. In such studies, the stability will probably depend on the Reynolds number and Froude number as well as the Weber number.

The sinuous and varicose modes of curtain waves predicted by Lin were found in thin liquid curtains and the thin parts of thick liquid curtains. Excellent agreements have been found between the theory and experiments. The angle between the tangent to the curve of constant phase of sinuous waves and the vertical has been successfully exploited to determine the dynamic surface tension. The difference between the dynamic and the static surface tensions was found to be not measurable for a pure liquid but very significant for a liquid solution. A plausible explanation has been given for the observed significant difference. Careful studies of the diffusion toward and adsorption at the free surface of the solute may contribute to a better understanding of the physical nature of the dynamic surface tension.

The authors wish to thank Dr O. T. Bloomer and Dr M. G. Antoniades of Eastman Kodak Company for useful suggestions and discussions. This work was completed while S. P. Lin was on a sabbatical leave with the Chemical Engineering Department at the University of Rochester. Thanks are due them for providing a congenial and hospitable atmosphere.

REFERENCES

ANTONIADES, M. G. & LIN, S. P. 1980 *J. Colloid Interface Sci.* **77**, 583.
BROWN, D. R. 1961 *J. Fluid Mech.* **10**, 297.
LIN, S. P. 1981 *J. Fluid Mech.* **104**, 111.
RAYLEIGH, Lord 1893 *Proc. Lond. Math. Soc.* **15**, 69.
SAVART, F. 1833 *Annls Chim. Phys.* **59**, 55 and 113.
THOMAS, W. D. E. & POTTER, L. 1975 *J. Colloid Interface Sci.* **50**, 397.
TAYLOR, G. I. 1959 *Proc. Roy. Soc.* A **253**, 289.
TAYLOR, G. I. 1960 *Proc. Roy. Soc.* A **259**, 1.